THE JOURNAL OF COMPARATIVE NEUROLOGY 444:144–158 (2002)

# Cortical Projections to the Nucleus of the Optic Tract and Dorsal Terminal Nucleus and to the Dorsolateral Pontine Nucleus in Macaques: A Dual Retrograde Tracing Study

CLAUDIA DISTLER,[1]* MICHAEL J. MUSTARI,[2] AND KLAUS-PETER HOFFMANN[1]
[1]Allgemeine Zoologie & Neurobiologie, Ruhr-Universität Bochum, 44780 Bochum, Germany
[2]Yerkes Regional Primate Center, Department of Neurology, Atlanta, Georgia 30322

ABSTRACT

The nucleus of the optic tract and dorsal terminal nucleus of the accessory optic system (NOT-DTN) along with the dorsolateral pontine nucleus (DLPN) have been shown to play a role in controlling slow eye movements and in maintaining stable vision during head movements. Both nuclei are known to receive cortical input from striate and extrastriate cortex. To determine to what degree this cortical input arises from the same areas and potentially from the same individual neurons, we placed different retrograde tracers into the NOT-DTN and the DLPN. In the ipsilateral cortical hemisphere the two projections mainly overlapped in the posterior part of the superior temporal sulcus (STS) comprising the middle temporal area (MT), the middle superior temporal area (MST), and the visual area in the fundus of the STS (FST) and the surrounding cortex. In these areas, neurons projecting to the NOT-DTN or the DLPN were closely intermingled. Nevertheless, only 3–11% of the labeled neurons in MT and MST were double-labeled in our various cases. These results indicate that the cortical input to the NOT-DTN and DLPN arises from largely separate neuronal subpopulations in the motion sensitive areas in the posterior STS. Only a small percentage of the projection neurons bifurcate to supply both targets. These findings are discussed in relation to the optokinetic and the smooth pursuit system. J. Comp. Neurol. 444:144–158, 2002. 

**Indexing terms: optokinetic reflex; smooth pursuit; cortico-pretectal; cortico-pontine; superior temporal sulcus; pulvinar; laminar distribution**

Slow eye movements are essential to stabilize the image of the world on the retina to compensate for self-motion and movement of the visual world. There is accumulating evidence that the neuronal basis for these eye movements is distributed over visual cortical areas in addition to distinct pretectal and brainstem nuclei from where the visual information is transferred to the cerebellum and further oculomotor structures. Traditionally, the nucleus of the optic tract and the dorsal terminal nucleus of the accessory optic system (NOT-DTN) are regarded as the key visuomotor interface for the optokinetic reflex that stabilizes large field retinal image motion or slip on the retina. The dorsolateral pontine nucleus (DLPN) has been largely implicated in slow eye movements during smooth pursuit of small stimuli and in the ocular following response (OFR).

The NOT is a functionally inhomogeneous structure containing several types of neurons that differ both in their response properties and their efferent projections. In cats, physiologically, at least three types of neurons have been identified: retinal slip neurons that are directionally selective for ipsiversive image motion (see below) and

Grant sponsor: Deutsche Forschungsgemeinschaft SFB509 NIH; Grant number: NEI EY06069.

*Correspondence to: Claudia Distler, Allgemeine Zoologie & Neurobiologie, Ruhr-Universität Bochum, Postfach 102148, D-44780 Bochum, Germany. E-mail: distler@neurobiologie.ruhr-uni-bochum.de

Received 28 June 2001; Revised 12 October 2001; Accepted 7 November 2001


DOI 10.1002/cne.10127

project to the dorsal cap of the inferior olive (e.g., Hoffmann and Schoppmann, 1975; Hoffmann et al., 1988); jerk neurons that respond to saccade-like stimulus movement (e.g., Ballas and Hoffmann, 1985) and project to the lateralis posterior nucleus of the thalamus (Sudkamp and Schmidt, 1995); and saccade neurons that are slightly direction selective, activated during saccades, and project to the lateral geniculate nucleus (Schmidt, 1996).

In monkeys, in addition to the retinal slip neurons (Hoffmann et al., 1988; Mustari and Fuchs, 1990) omnidirectional pause neurons anatomically clearly offset with respect to the retinal slip neurons have been described in the nucleus of the optic tract (Mustari et al., 1997). For the DTN, only retinal slip neurons have been described in cats (Grasse and Cynader, 1984) and monkeys (Hoffmann et al., 1988; Mustari and Fuchs, 1990). For the purpose of this and previous studies, we consider the retinal slip neurons in the NOT and DTN as a functional unit because, first, in our experience, they cannot be distinguished based on their response properties, their orthodromic latencies from the retina or the visual cortex, their antidromic latencies from the inferior olive (Hoffmann et al., 1988), or their antidromic latencies to cortex (Hoffmann et al., 2002), and second, their distribution and morphology after retrograde labeling from the inferior olive appears homogeneous. Although we do not deny some cytoarchitectonic differences between the NOT as a whole and the DTN as described by Büttner-Ennever and coworkers (Büttner-Ennever et al., 1996b), for the sake of brevity, in this and related studies, we define retinal slip neurons in the NOT and the DTN as NOT-DTN neurons and their location as the NOT-DTN.

As in all other mammals investigated to date, retinal slip neurons in the monkey NOT-DTN respond preferentially during large field visual motion toward the side of recording (ipsiversively) (Hoffmann et al., 1988; Mustari and Fuchs, 1990). In addition, some NOT-DTN neurons also respond to small spots of light moving ipsiversively (Hoffmann and Distler, 1989; Mustari and Fuchs, 1990; Ilg and Hoffmann, 1991) that elicit smooth eye movements in awake animals. Electrical stimulation in the NOT-DTN leads to optokinetic eye movements with the slow phase toward the stimulated side (Schiff et al., 1988; Mustari and Fuchs, 1990; Taylor et al., 2000; Hoffmann and Fischer, 2001). Similarly, lesion or inactivation of the NOT-DTN leads to deficits of optokinetic eye movements during visual stimulation toward the lesion (Kato et al., 1988; Schiff et al., 1990; Ilg et al., 1993; Inoue et al., 2000; Hoffmann and Fischer, 2001). Interestingly, lesions of the NOT-DTN also impair smooth pursuit (Ilg et al., 1993; Yakushin et al., 2000b). Thus, the NOT-DTN in the monkey not only plays an important role for the optokinetic nystagmus but for all slow eye movements.

In the DLPN, several types of neurons have been found, including purely visual, eye movement-related, and visual-pursuit neurons. The visual and visual-pursuit neurons respond to moving large area random dot patterns, and, in part, to moving single spots of light in a direction selective manner. In contrast to the NOT-DTN, these neurons as a population do not code for a common direction of movement (Suzuki and Keller, 1984; Mustari et al., 1988; Thier et al., 1988; Suzuki et al., 1990). Especially the eye movement-related and visual-pursuit neurons have implicated the DLPN in the smooth pursuit pathway. Lesion of the DLPN causes impairment of smooth pursuit and of the initial phase of optokinetic eye movements, whereas the steady-state optokinetic response is unaffected (May et al., 1988; Thier et al., 1991). In addition, Kawano and coworkers described DLPN neurons that fire before eye movements and whose response properties show a similar stimulus dependence as ocular following, thus implicating these neurons in OFR (Kawano et al., 1992, 1996).

Within the cerebral cortex, pursuit-related neurons have been identified in several cortical areas, including the frontal eye fields, the lateral intraparietal area, and the superior temporal areas MT and MST. In MT and MST, these direction selective neurons include the representation of the fovea in their receptive fields but differ in their preferred stimulus and receptive field size, with MT neurons having smaller receptive fields and preferring small instead of large area visual stimuli (Komatsu and

*Abbreviations*

| | |
|---|---|
| A | aqueduct |
| amt | anterior mediotemporal sulcus |
| ar | arcuate sulcus |
| BSC | brachium of the superior colliculus |
| ca | calcarine sulcus |
| ce | central sulcus |
| ci | cingulate sulcus |
| CTB | choleratoxin subunit B |
| DLPN | dorsolateral pontine nucleus |
| DMZ | densely myelinated zone of MST |
| DTN | dorsal terminal nucleus of the accessory optic system |
| DPC | decussatio pedunculorum cerebellaris superiorum |
| DY | Diamidino Yellow |
| FEF | frontal eye field |
| FST | visual area at the floor of the superior temporal sulcus |
| FLM | fasciculus longitudinalis medialis |
| GB | Granular Blue |
| io | inferooccipital sulcus |
| ip | intraparietal sulcus |
| la | lateral sulcus |
| LIP | lateral intraparietal area |
| LL | lemniscus lateralis |
| lu | lunate sulcus |
| MGN | medial geniculate nucleus |
| MT | middle temporal area |
| MST | middle superior temporal area |
| MVN | medial vestibular nucleus |
| NOT | nucleus of the optic tract |
| NPH | nucleus prepositus hypoglossi |
| NRTP | nucleus reticularis tegmenti pontis |
| ot | occipitotemporal sulcus |
| p | principal sulcus |
| PAG | periaqueductal grey |
| PCM | pedunculus cerebellaris medialis |
| pom | middle parieto-occipital sulcus |
| Pul | pulvinar |
| RD | rhodamine dextrane |
| SC | superior colliculus |
| STS, st | superior temporal sulcus |
| TMB | tetramethylbenzidine |
| TG | cortical area TG |
| TP | tractus pyramidalis |
| V1 | primary visual cortex |
| V4t | transitional zone of visual area 4 |
| VIP | ventral intraparietal area |
| WGA-HRP | horseradish peroxidase coupled to wheat germ agglutinin |

Wurtz, 1988). Lesions in MT produce a retinotopic deficit in smooth pursuit, whereas MST lesions lead to retinotopic as well as directional deficits in smooth pursuit and the slow buildup of optokinetic nystagmus (OKN; Newsome et al., 1985; Duersteler and Wurtz, 1988). Area MST also contains neurons related to ocular following (Kawano et al., 1994). Both MT and MST project to the DLPN (e.g., Maunsell and Van Essen, 1983; Ungerleider et al., 1984; Boussaoud et al., 1992). The main cortical input to the NOT-DTN comes from MT (Distler and Hoffmann, 2001).

The aim of the present investigation was to determine the relative contributions of MT and MST to the cortical projections to NOT-DTN and DLPN and whether the same individual neurons provide input to both targets. In addition, we investigated whether there are other cortical areas providing input to both NOT-DTN and DLPN.

TABLE 1. Summary of Experimental Design[1]

| Case | Species | Injection site | Tracer | Volume (μl) | Survival |
|---|---|---|---|---|---|
| 1 | *M. fascicularis* | Right MT | WGA-HRP | 0.15 | 48h |
| 2 | *M. mulatta* | Right NOT | CTB | 0.4 | 3d |
| | | Right DLPN | WGA-HRP | 0.1 | 3d |
| 3 | *M. fascicularis* | Right NOT | GB | 0.15 | 8d |
| | | Right DLPN | DY | 1.0 | 8d |
| 4 | *M. fascicularis* | Right NOT | DY | 1.1 | 10d |
| | | Right DLPN | GB | 0.15 | 10d |
| 5 | *M. fascicularis* | Left NOT | CTB | 0.7 | 4d |
| | | Left DLPN | WGA-HRP | 0.15 | 4d |
| Pul1 | *M. mulatta* | Right Pul dors. | RD | 0.5 | 4d |
| Pul2 | *M. mulatta* | Right Pul med. | CTB | 0.05 | 4d |
| Pul3 | *M. mulatta* | Right Pul | WGA-HRP | 0.05 | 4d |
| Pul4 | *M. mulatta* | Right Pul/MGN | CTB | 0.3 | 4d |
| NRTP | *M. mulatta* | Left NRTP | RD | 0.25 | 4d |

[1]h, hour; d, day; dors., dorsal; med., medial. for other abbreviations, see list.

## MATERIALS AND METHODS

### Subjects

All experiments of this study were carried out in accordance with the European Communities Council Directive of 24 November 1986 (86 609 EEC) and NIH guidelines for care and use of animals for experimental procedures and had been approved by the local ethics and Institutional Animal Care and Use committee. Altogether, 13 tracer injections were performed in adult macaques (two female, one male *Macaca fascicularis*, three male *M. mulatta*).

### Surgery and injections

The female M. fascicularis were initially anesthetized with ketamine hydrochloride (10 mg/kg i.m.), intubated, and received an intravenous catheter before being placed into the stereotaxic apparatus. After additional local anesthesia with bupivacaine hydrochloride (Bupivacain, 0.5 ml) or prilocaine hydrochloride 0.5% (Xylonest, 0.5 ml), the skin overlying the skull was cut and a craniotomy was performed to allow access to the pretectum and to the pontine nuclei. During surgery, the animals were artificially ventilated with nitrous oxide: oxygen as 3:1 containing 0.3%–1% halothane. In addition, they received doses of pentobarbital as needed. Heart rate, $SPO_2$, blood pressure, body temperature, and end tidal $CO_2$ were constantly monitored and kept at physiological levels.

Retinal slip neurons in the NOT-DTN were localized in perpendicular penetrations based on their location lateral and anterior to the foveal representation in the superior colliculus and on their characteristic preference for ipsiversive stimulus movement (Hoffmann et al., 1988). For localizing the DLPN, the electrode was angled 20 degrees from the contralateral side. The DLPN was then identified based on its stereotaxic location and on the prevalence of direction selective neuronal responses (Mustari et al., 1988). When a putative injection site was localized, the recording electrode was replaced with a glass pipette containing a recording wire. The pipette was connected by means of a short tube to a Hamilton syringe. Before the injection, the previously recorded response properties were verified. Then, 4% Diamidino Yellow (DY) (EMS-Polyloy, Groβ-Umstadt, Germany) in distilled water, 2% Granular Blue (GB) (EMS-Polyloy) in distilled water, 15% rhodamine dextran (RD) (MW 3000) (Molecular Probes, Leiden, Netherlands) in 0.1 M citrate-NaOH, pH 3.0, 2% wheat germ agglutinin conjugated to horseradish peroxidase (WGA-HRP) (Sigma, Munich, Germany) in 0.1 M phosphate buffer pH 7.4, or 1% cholera toxin subunit B (CTB) (Quadratech, Epsom, UK) in distilled water was slowly injected over a 30-minute time period (Table 1). After 20 minutes, the pipette was withdrawn after aspiration to minimize leakage of the tracer into the overlying tissue. After completion of the injections, the wound was closed in appropriate layers and the animals were allowed to recover. Animals were treated prophylactically with broad-spectrum antibiotics and analgesics until they were sacrificed.

The procedures for training and chronic implantation of the remaining animals are described in detail elsewhere (Mustari et al., 1994; Thiele et al., 1997). In short, animals were trained to fixate a small diameter (0.1 degree) target spot at various eccentricities, to perform smooth pursuit to step-ramp target motion, and to make saccades to target steps. To localize the NOT-DTN, the NRTP, and the DLPN, single units were recorded during fixation, smooth pursuit, and saccades. During fixation, a large field random dot pattern (100 degree × 100 degree) was projected on a tangent screen 57 cm in front of the animal and moved in eight cardinal directions spaced 45 degrees apart to identify direction selective visual neurons in the NOT-DTN, NRTP, and DLPN. Once these nuclear groups were identified, the electrode was replaced with a glass pipette, and tracers were pressure injected by using a pico-pump (WPI-PV830).

Altogether, four pairs of injections with different tracers were placed in the NOT-DTN and DLPN. In addition, control injections were placed into the NRTP (one case) and various parts of the pulvinar (four cases). The location, the tracer, the amount of tracer, and the survival times for the individual cases are summarized in Table 1.

### Histology

After appropriate survival time, the animals were sedated with ketamine hydrochloride and sacrificed with an overdose of pentobarbital (80–100 mg/kg). Then they were perfused through the heart with 0.9% NaCl containing 0.1% procaine hydrochloride, followed by paraformaldehyde-lysine-periodate containing 4% paraformaldehyde. After post-fixation overnight, the tissue was transferred to 0.1 M PB containing 10% glycerol followed by 20% glycerol for cryoprotection.

The midbrains were cut in the coronal stereotaxic plane at 50 μm. At least two alternate series were cut, one was

used for visualization of the injection sites, the other set was Nissl stained for identification of midbrain nuclei. The cortical hemispheres were cut at 50 μm in the frontal (three cases) or the parasagittal plane (five cases). Five alternate series were cut: one or two series were used for visualization of retrogradely labeled cells, additional series were used for Nissl staining, myeloarchitecture, SMI 32-, and *Wisteria floribunda* agglutinin histochemistry (Gallyas, 1979, as modified by Hess and Merker, 1983; Brückner et al., 1994; Hof and Morrison, 1995).

For visualization of fluorescent tracers, the sections were mounted from 0.45% NaCl immediately after cutting, dried on a hot plate, defatted in fresh xylene (2 × 1 minute), and cover-slipped with DEPEX. Tetramethylbenzidine (TMB) was used for visualization of WGA-HRP (after van der Want et al., 1997). For double labeling with cholera toxin, the TMB reaction product was first stabilized with ammonium heptamolybdate followed by a second stabilization with diaminobenzidine. Then, CTB immunohistochemistry was performed and CTB was visualized with streptavidin coupled to CY3 or CY2 (modified after Angelucci et al., 1996).

### Data analysis

Retrogradely labeled neurons were viewed with a fluorescence microscope (Zeiss Axioskop) and charted on enlarged drawings of the entire ipsilateral cortical hemisphere at 1-mm interval. In cases with very limited labeling, data were plotted at 250-μm intervals. Cortical areal borders were determined based on the myeloarchitectonic characteristics and SMI-32 label as described in the literature. The location of retrogradely labeled cells and areal borders were then transferred onto two-dimensional maps derived from physically constructed three-dimensional wire models (Van Essen and Maunsell, 1980; Distler et al., 1993).

To quantify the occurrence of double-labeled cells in relation to the overall number of neurons labeled after NOT-DTN or DLPN injections, we counted labeled cells and expressed their density as cells per mm in layer V in areas MT and MST of the four dual tracer cases. Similarly, the density of labeled cells found in layers V and VI was determined and compared between NOT-DTN, DLPN, and pulvinar-cases to judge the involvement of structures neighboring our injection sites (see Tables 1 and 4).

Retrogradely labeled neurons, anterogradely labeled axon terminals, and injection sites were documented with a photomicroscope (ZEISS Axiophot) by using a Tmax 100 or an Kodak Ectachrome 400 film.

## RESULTS

### Cortical label in NOT-DTN and DLPN

***Case 1.*** During the course of otherwise unrelated electrophysiological recordings in area MT of an awake monkey, neurons were identified that were direction selective for ipsiversive stimulus movement and had large receptive fields that reached beyond the fovea into the ipsilateral visual hemifield, thus, strongly resembling neurons projecting to the NOT-DTN (Hoffmann et al., 1992; Ilg and Hoffmann, 1993). Even though in this case no antidromic identification was performed, an iontophoretic WGA-HRP injection at such a recording site yielded a small but clear projection to the NOT-DTN and to the DLPN. Figure 1 includes line drawings of a section taken through our cortical injection site (Fig. 1A) and sections through the NOT-DTN (Fig. 1C) and DLPN (Fig. 1E). Anterograde label is indicated by stippling on the line drawings. The rectangles indicate the respective areas shown enlarged in the darkfield photomicrographs in Figure 1B,D, and F. Arrows point to anterogradely labeled cortical terminals.

### Retrograde label in cortical areas

In two cases, we performed small tracer injections at recording sites of retinal slip neurons in the NOT-DTN and in the DLPN. Such injections were almost completely restricted to their respective target but may not have covered the entire nucleus. These cases allow us to determine whether the same individual neurons project to the NOT-DTN and the DLPN or if there are separate subpopulations projecting to one or the other target. In two more cases, rather large injections into the NOT-DTN and the DLPN were made to cover the whole nuclei with tracer even if compromising on the absolute specificity of the injections. Such large injections allowed us to estimate the maximum possible extent of overlapping projections and number of double-labeled neurons.

Figure 2 shows fluorescent photomicrographs of some examples of retrogradely labeled cells in the STS of case 5. These neurons were located in cortical layer V. Such neurons were typical pyramidal cells and in most cases at least the proximal portions of the apical and basal stem dendrites were visible. However, we did not analyze the arborization pattern of these neurons in detail. Note that neurons labeled after NOT-DTN injection (red fluorescence) and neurons labeled after pontine injection (black staining) lie intermingled and very close to each other. There was no obvious clustering of neurons projecting to one or the other target. Only rarely were individual neurons labeled from both injection sites (arrow in Fig. 2C).

***Case 2.*** The smallest injections in this series were placed in case 2. The CTB injection into the NOT-DTN extended approximately 500 μm anterior-posteriorly and did not discernibly involve pulvinar or superior colliculus. The pontine injection with WGA-HRP was centered in the lateral NRTP and the DLPN and extended 500–900μm anterior-posteriorly (Fig. 3B).

A summary of the cortical label found in case 2 is given in Table 2. The strength of labeling is indicated semiquantitatively within an individual case by classifying it as strong (+++), moderate (++), light (+), or scattered (±). In addition, the shaded parts in Table 2 indicate the areas where the label resulting from the NOT-DTN and the DLPN injections consistently coincided. Outside the STS, the strongest label after NOT-DTN injection was in area TG, mainly in layer VI, and also in the frontal eye field (FEF), the posterior bank of the arcuate sulcus, and in V1. In the latter areas, label was restricted to layer V. Moderate to scattered label was present in V2-V4 (compare also Distler and Hoffmann, 2001). The pontine injection yielded strong label in ventral intraparietal area (VIP) and PO. The only area of overlap of the two projections was the posterior part of the STS, areas MT and MST (Fig. 3C).

Figure 3A shows the two-dimensional map of the right STS of case 2. In this and the following figures, neurons labeled after NOT-DTN injections are represented by red dots, those labeled by DLPN injections are represented by blue dots, regardless of the tracers used. Double-labeled

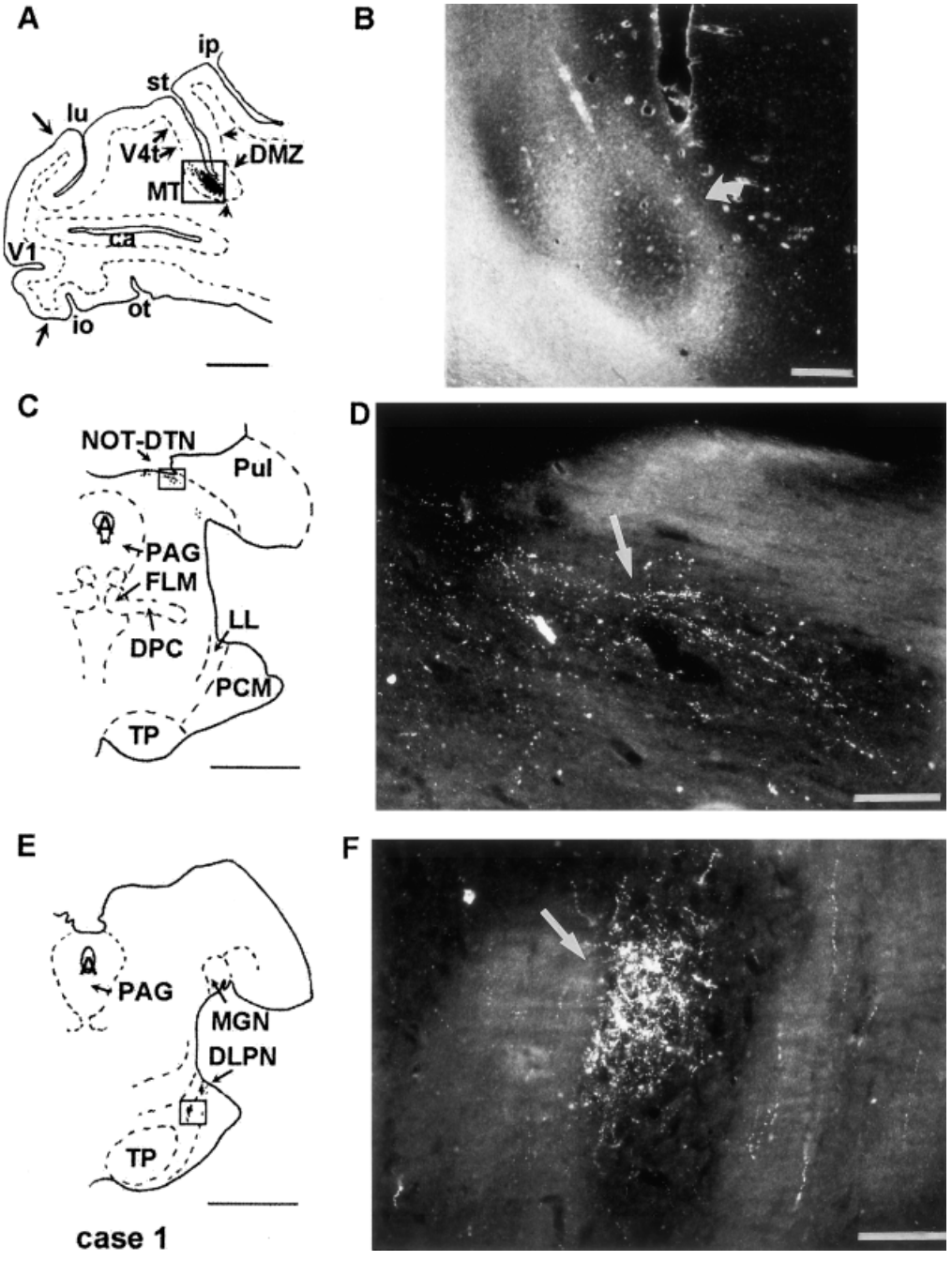


Fig. 1. Anterogradely labeled terminals and fibers in the NOT-DTN (**C,D**) and the DLPN (**E,F**) after a WGA-HRP injection into area MT (**A,B**) of case 1. The insets in the line drawings in A,,C,E indicate the region depicted in the darkfield microphotographs in B,D,F, respectively. Arrows point to the injection site in B and to labeled terminals in D,F. For abbreviations, see list. Scale bars = 5 mm in A,C,E, 2 mm in B, 100 μm in D,F.

cells are indicated by green dots. The density of the dots semiquantitatively indicates the density of labeled cells. The location and the layer distribution of labeled cells in the entire cortical hemisphere is indicated by the 3 representative sections shown in Figure 3C. Only one double-labeled cell was found in this case. It was located in MST (Table 3).

***Case 3.*** This case received a GB injection (anterior-posterior extent 1–1.5 mm) centered in the NOT-DTN without any discernible involvement of the pulvinar but possibly including the very edge of the superior colliculus. The pontine injection with DY (anterior-posterior extent 2.5 mm) was centered in the NRTP but also included substantial parts of the DLPN (Fig. 4B). In

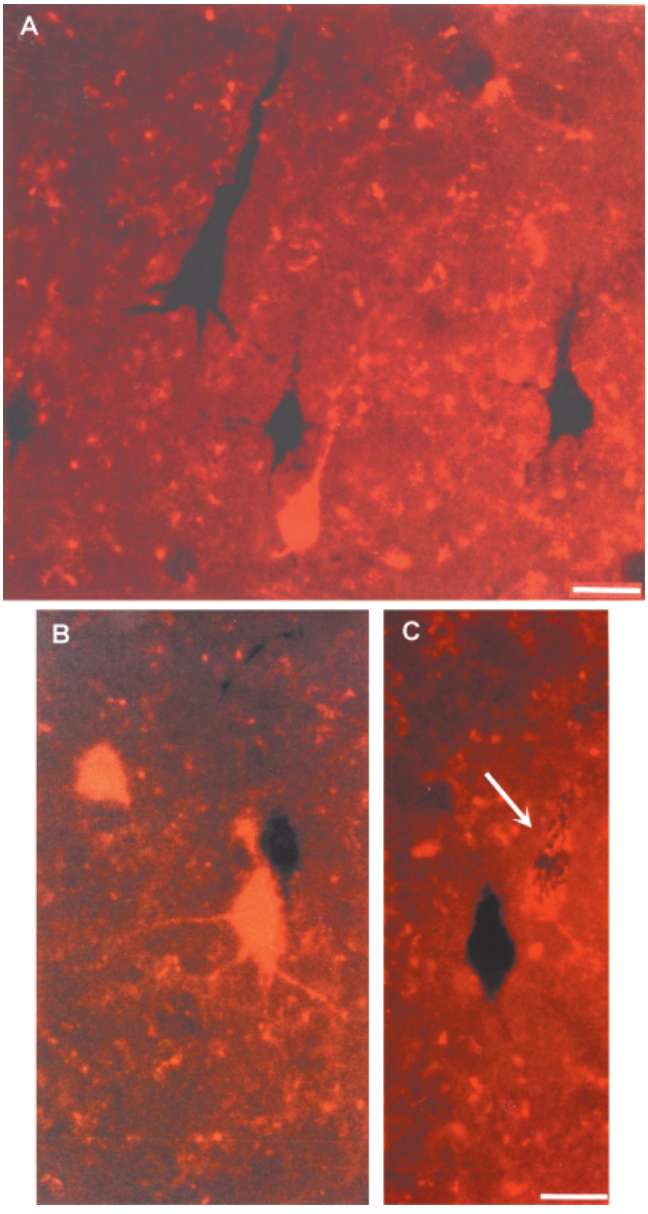


Fig. 2. Photomicrographs of neurons retrogradely labeled after WGA-HRP injection into the DLPN (black) and CTB injection into the NOT-DTN (red) of case 5. The arrow in C points to a double-labeled neuron. For abbreviations, see list. Scale bar = 25 μm in A,C (applies also to B).

this case, labeled cells were found in the ipsilateral NOT-DTN.

The resulting cortical label is documented on the 2-D map of the STS (Fig. 4A) and on the representative cortical sections depicted in Figure 4C. The strongest label from the NOT-DTN injection outside the STS was in TG and, as in the other cases, it was mainly located in layer VI. In the other cortical areas, label was located in layer V only. Outside the STS, only areas V1 to V4 were labeled in this case. The pontine injection labeled the cingulate and principal sulci, the FEF, and to a lesser degree orbital cortex, TG, and the anterior bank of the intraparietal sulcus. In this case, the only area of overlap was the posterior part of the STS, mainly comprising areas MT, MST, and FST.

Despite the good overlap in these areas, only two double-labeled cells were found in the entire hemisphere both of which were located in MT. They represent 2.9% of the NOT-DTN–projecting neurons and 3.4% of DLPN projecting neurons in MT (Table 3).

***Case 4.*** This case received a DY injection into the NOT-DTN that also involved part of the lateral pulvinar and extended approximately 2.5 mm anterior-posteriorly. The pontine injection with GB extended 3–4 mm anterior-posteriorly and involved the DLPN, the NRTP, and the lateral pons (Fig. 5B). As in case 3, retrogradely labeled cells were found in the ipsilateral NOT-DTN.

Outside the STS the strongest label after NOT-DTN injection was again in TG and the adjoining upper bank of the STS. Moderate label was found in V1 and V2, light label was present in V3, V4, PO, the lateral sulcus, the posterior bank of the intraparietal sulcus, the principal sulcus, and the orbital cortex. By contrast, the pontine injection yielded moderate label in PO and the anterior bank of the intraparietal sulcus and light label in the lateral and cingulate sulci, in LIP, VIP, FEF, and the orbital cortex. Scattered labeled cells were located in TG and the principal sulcus. The region with the most significant overlap of neurons labeled after NOT-DTN and DLPN injections was the posterior part of the STS. Both labels were moderate to strong in areas MT, MST, and FST (Fig. 5A; Table 2). Figure 5C emphasizes the overlap of NOT-DTN– and DLPN- neurons mainly in the STS followed by the intraparietal sulcus and the PO area. Neurons labeled from the DLPN were always located in layer V, whereas the NOT-DTN injection yielded a bilaminar distribution of labeled cells in layers V and VI in the middle parieto-occipital sulcus (pom), area 7a in the posterior bank of the intraparietal sulcus, and in some parts of the STS (see below).

In the entire cortical hemisphere, 47 double-labeled cells were found, all of which were located in layer V. Of these neurons, 11 were located in MT, 9 were in MST, 4 in FST, 7 were found in the cortex surrounding MT and MST, 10 were found in the intraparietal sulcus, and 6 were in the pom. The double-labeled neurons in MT constituted 3.3% of the NOT-DTN–projecting cells and 10.4% of the DLPN-projecting cells. In MST, 3.4% of the NOT-DTN–projecting cells and 3.9% of the DLPN-projecting cells were double-labeled (Table 3).

***Case 5.*** The largest injections were placed in case 5. Although the exact extent of the CTB injection site cannot be delineated due to technical difficulties during histologic processing, the center of the injection as determined by the pipette track certainly was located in the NOT-DTN. Note that only this center is marked in the reconstruction of the injection site in Figure 6B. Leakage of tracer into the white matter or medial cortex was not evident. However, the tracer probably spread to neighboring structures as the medial and lateral pulvinar, the medial geniculate nucleus, the suprageniculate nucleus, and the pretectal olivary nucleus. This explanation would account for the presence of labeled cells found in frontal and orbital cortex, the anterior cingulate, as well as in the auditory cortex (Table 2).

The WGA-HRP injection in case 5 was centered at the border between NRTP and DLPN, its anterior-posterior

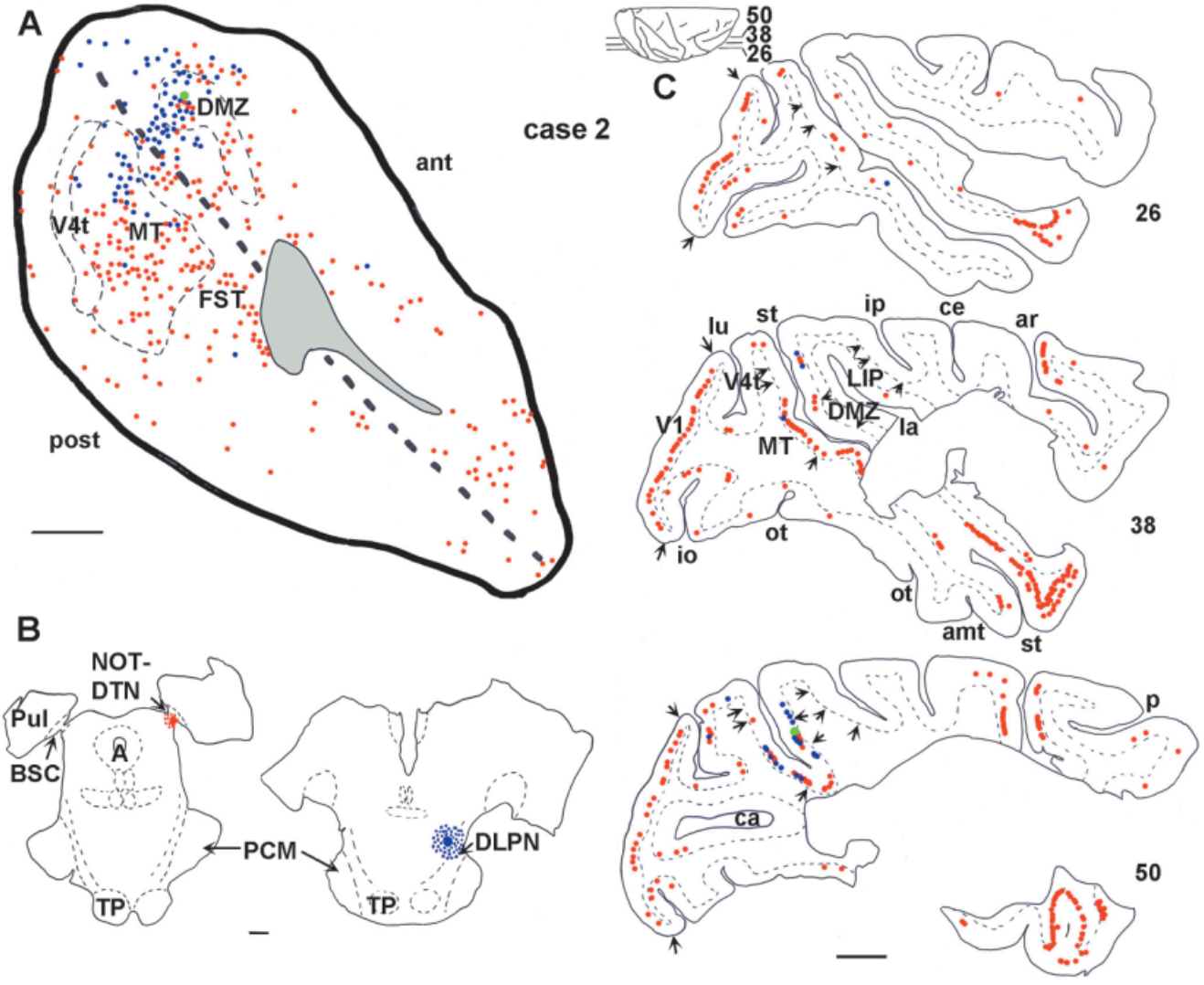


Fig. 3. The injection sites (**B**) and the resulting retrograde label in the ipsilateral STS as shown on a two-dimensional map of the right hemisphere derived from parasagittal sections (**A**) of case 2. Red dots represent neurons labeled after NOT-DTN injection, blue dots represent cells labeled by DLPN injection, green dot represents a double-labeled neuron. Only neurons in layer V are represented on this map. The thick dashed line indicates the fundus of the sulcus; thin dashed lines indicate myeloarchitectonic borders. The shaded area in the STS map represents tissue lost in dissection. **C:** Line drawings of representative sections of case 2 demonstrating the location and layer distribution of labeled neurons outside the STS. Dashed lines indicate the border between gray and white matter; arrows point to myeloarchitectonic borders. The location of the sections in the brain is indicated in the inset. ant, anterior; post, posterior. For other abbreviations see list. Scale bars = 2 mm in B, 5 mm in A,C.

extent amounted to approximately 4 mm (Fig. 6B). Even though the midbrain connections were not investigated in detail, also this injection yielded some retrogradely labeled cells in the ipsilateral NOT-DTN.

Outside the STS, neurons retrogradely labeled by the NOT-DTN injection were found in V1, V2, V3, and V4, in areas LIP, VIP, and in the anterior bank of the intraparietal sulcus, in area PO, in area TG and the anterior part of the lower bank of the lateral sulcus, in the FEF, in the anterior part of the cingulate sulcus, in the principal sulcus, and in the orbital cortex. By contrast, the pontine injection did not yield any label in the primary visual areas (V1–V4), area TG, the lateral, cingulate, or principal sulcus or the orbital cortex. Outside the STS, consistent labeling was found in LIP, VIP, and in the anterior bank of the intraparietal sulcus, in PO and FEF. The most significant overlap resulting from the two injections was found in the posterior STS, mainly in areas MT and MST and the surrounding cortex. In addition, overlapping label was found in FEF and LIP (Fig. 6A,C).

Note that, in the most lateral part of the anterior bank of the STS and in area TG, labeling originating from the NOT-DTN injection is bilaminar with a clear preponderance of layer VI label. Labeling in the frontal and orbital cortex was almost exclusively found in layer VI. By contrast, in areas identified as the prime NOT-DTN–projecting structures (MT, V1, V2, V3; Distler and Hoffmann, 2001) and in area MST labeled neurons were found

TABLE 2. Summary of Cortical Areas Labeled After NOT-DTN and After DLPN Injections[1]

| Area | Case 2 NOT-DTN | Case 3 NOT-DTN | Case 4 NOT-DTN | Case 5 NOT-DTN | Case 2 DLPN | Case 3 DLPN | Case 4 DLPN | Case 5 DLPN |
|---|---|---|---|---|---|---|---|---|
| V1 | +++ | ++ | ++ | ++ | − | − | − | − |
| V2 | ± | + | ++ | + | − | − | − | − |
| V3 | + | + | + | + | − | − | − | − |
| V4 | ± | ± | + | + | ± | − | − | − |
| PO | − | − | + | + | ++ | − | ++ | + |
| MT | ++ | ++ | ++ | ++ | + | ++ | ++ | ++ |
| MST | + | ++ | ++ | ++ | ++ | ++ | +++ | +++ |
| FST | + | + | +++ | ++ | − | ± | ++ | + |
| STS ant upper b. | ++ | ± | +++ | +++ | − | − | + | − |
| STS ant lower b. | ± | + | +++ | ++ | − | − | − | − |
| TG | +++ | +++ | +++ | +++ | − | ± | ± | − |
| Lateral | −/0 | − | + | ++ | −/0 | − | + | − |
| LIP | − | − | + | ++ | − | − | + | ++ |
| VIP | − | − | + | + | ++ | − | + | + |
| ip ant | − | − | − | + | ± | ± | ++ | ++ |
| FEF | +++ | − | − | +++ | − | + | + | + |
| Principal | − | − | + | ++ | − | + | ± | − |
| Cingulate | − | − | − | ++ | − | ++ | + | − |
| Orbital | 0 | − | + | +++ | 0 | ± | + | − |

[1]Semiquantitative assessment of labeling strength after NOT-DTN and DLPN injections. +++, strong label; ++, moderate label; +, light label; ±, scattered label; −, no label; 0, not analyzed. STS ant upper b., upper bank of the anterior part of the STS; STS ant lower b., lower bank of the anterior part of the STS; ip ant, anterior bank of the intraparietal sulcus. For other abbreviations, see list.

TABLE 3. Quantification of Double-Labeled Neurons[1]

| Case | % of NOT-DTN in MT | % of DLPN in MT | % of NOT-DTN in MST | % of DLPN in MST |
|---|---|---|---|---|
| 2 | 0 | 0 | 8.3 | 11.1 |
| 3 | 2.9 | 3.4 | 0 | 0 |
| 4 | 3.3 | 10.4 | 3.4 | 3.9 |
| 5 | 3.4 | 3.9 | 9.6 | 4.3 |

[1]For abbreviations, see list.

predominantly if not exclusively in layer V (see also below).

Altogether, 15 double-labeled cells were found in the STS of case 5 amounting to 3.9% of the DLPN-projecting cells and 3.4% of the NOT-DTN–projecting cells in area MT, and to 4.3% of the DLPN-projecting cells and 9.6% of the NOT-DTN-projecting cells in area MST (Table 3). Three additional double-labeled cells were found, one in area LIPv and two in area V3A.

Thus, a common picture arises from these cases: the only consistent area of overlap of the two projection systems is located in areas MT and MST and the surrounding cortex. Averaged over all four cases and over MT and MST, 3.6% of NOT-DTN–projecting neurons and 4.7% of DLPN-projecting neurons were double-labeled, i.e., they project to both targets.

## Control injections

Especially cases 4 and 5 with rather large tracer injections merit a detailed analysis of the involvement of structures neighboring the injection sites. A recent analysis has shown that putative involvement of the superior colliculus can mainly be segregated from NOT-DTN injections based on the topographic relationship between injected collicular region and labeled cortical area (Distler and Hoffmann, 2001). In the present investigation, cases with larger NOT-DTN injections demonstrated label in cortical regions other than the typical NOT-DTN–projecting areas. In addition, quite often labeling in these areas was either bilaminar or predominantly in layer VI. Thus, to investigate to what extent involvement of structures surrounding our injections could influence our results, we analyzed the regional and laminar distribution of labeled neurons after pulvinar injections in four cases and after NRTP and medial pons injection in one case.

***Pulvinar injections.*** Figure 7 demonstrates the centers of the four pulvinar injections. Case Pul1 received a rather small rhodamine dextran injection in the dorsolateral part of the medial pulvinar, case Pul2 received a small CTB injection into the ventromedial part of the medial pulvinar just above the BSC. The WGA-HRP injection in case Pul3 was much larger, its halo included the medial pulvinar, the medial dorsal nucleus of the thalamus (Ungerleider et al., 1983), and parts of the NOT-DTN. The CTB injection in case Pul4 included the lateral pulvinar, parts of the medial geniculate nucleus, and the medial and centromedial subdivisions of the inferior pulvinar (Adams et al., 2000). Despite the variability in size and location of these injections, two characteristics could be recognized: first, each injection revealed multiple cortical input areas and, second, in most areas with the exception of area V1, this cortical projection to the pulvinar arose both from layers V and VI. The ratio of neurons labeled in layers V and VI varied between cortical areas as well as between injection sites. It was not the aim of the present study to analyze all cortical areas in detail. Thus, we concentrated on typical NOT-DTN input structures like the motion sensitive areas MT, MST, and FST and compared them with surrounding cortex. Table 4 summarizes the ratio of labeled cells in layers V and VI for various areas in all cases. It is evident that only the NOT-DTN cases with large injections (cases 4 and 5) show bilaminar label in the motion-sensitive areas as well as in the anterior part of the STS. In contrast, after small injections largely limited to the NOT-DTN (cases 2 and 3) cortical label was found exclusively in layer V (see also Distler and Hoffmann, 2001). With the exception of case Pul3, labeling in areas MT, MST, and FST was very sparse after pulvinar injection. The smaller injections in cases Pul1 and Pul2 resulted in a moderate to clear preponderance of

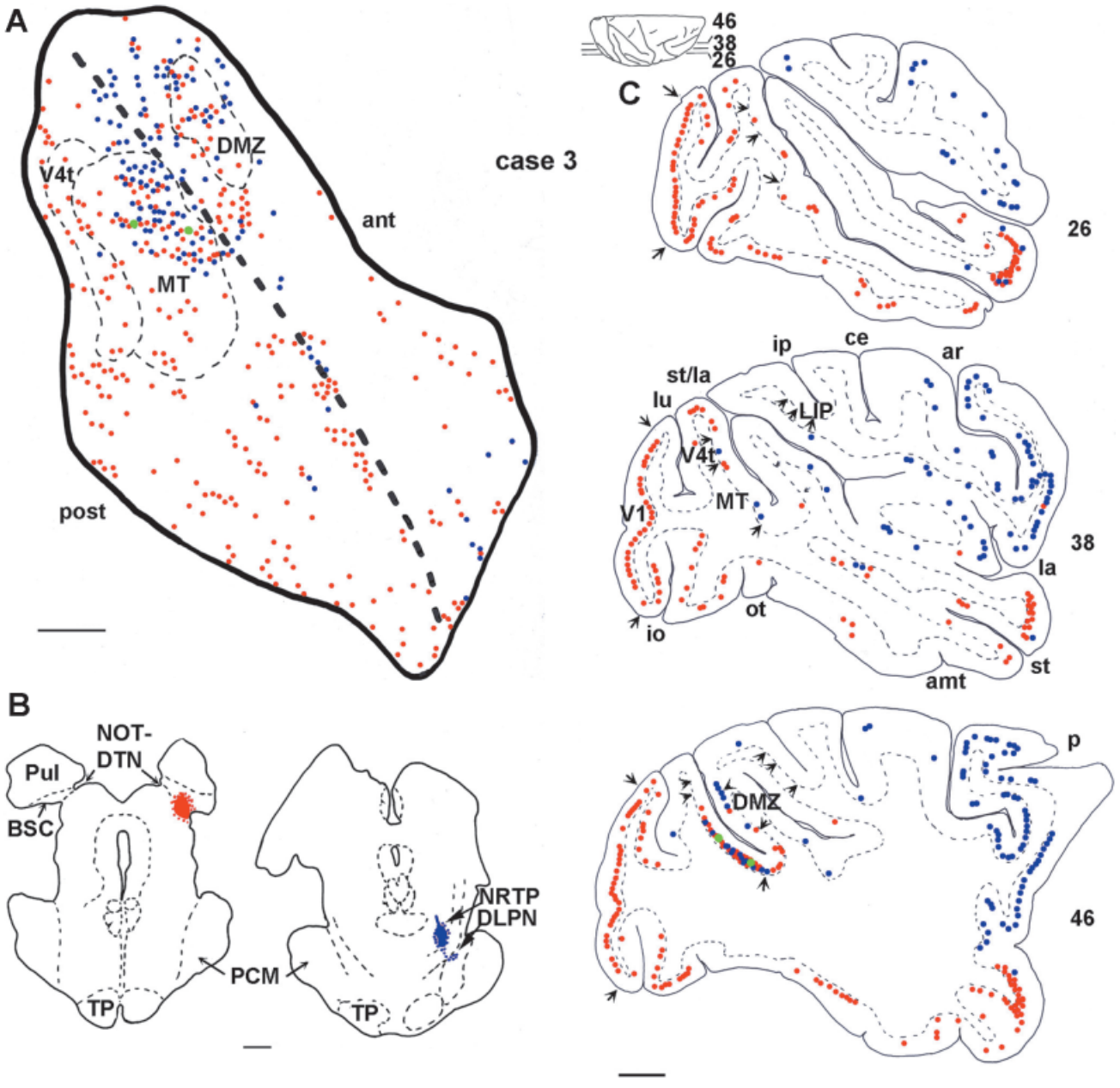


Fig. 4. Injections sites (**B**) and resulting retrograde label in the right hemisphere (**A,C**) of case 3. ant, anterior; post, posterior. For other abbreviations, see list. Other conventions as in Figure 3.

layer VI labeling in MT. In contrast, the larger injections in Pul3 and Pul4 resulted in heavier labeling in layer V. There was a clear preponderance of labeling in layer VI of areas MST and FST in all pulvinar cases and in NOT-DTN injection case 4. This labeling was only exceeded in the areas associated with the anterior part of the STS and in the lateral sulcus of case Pul4. Comparison of the pulvinar cases with our other NOT-DTN injection sites suggests that, in case 5, mainly the dorsomedial part of the medial pulvinar was involved. Similarly, in case 4, mainly the ventromedial part of the lateral pulvinar was involved in the NOT-DTN injection. Because both of these parts of the pulvinar do not represent main projection targets of MT (e.g., Adams et al., 2000), we conclude that involvement of the pulvinar in our NOT-DTN injections should make a negligible contribution to the labeling we find in layer V in our double labeling experiments. Therefore, our quantitative assessments of labeling intensity in layer V should offer a fair representation of NOT-DTN projections.

***NRTP injection.*** To judge the effect of involvement of the NRTP and medial pontine nuclei in our DLPN injections upon our cortical labeling, especially in the STS, we performed a control injection with rhodamine dextran (not demonstrated). This injection resulted in prominent label-

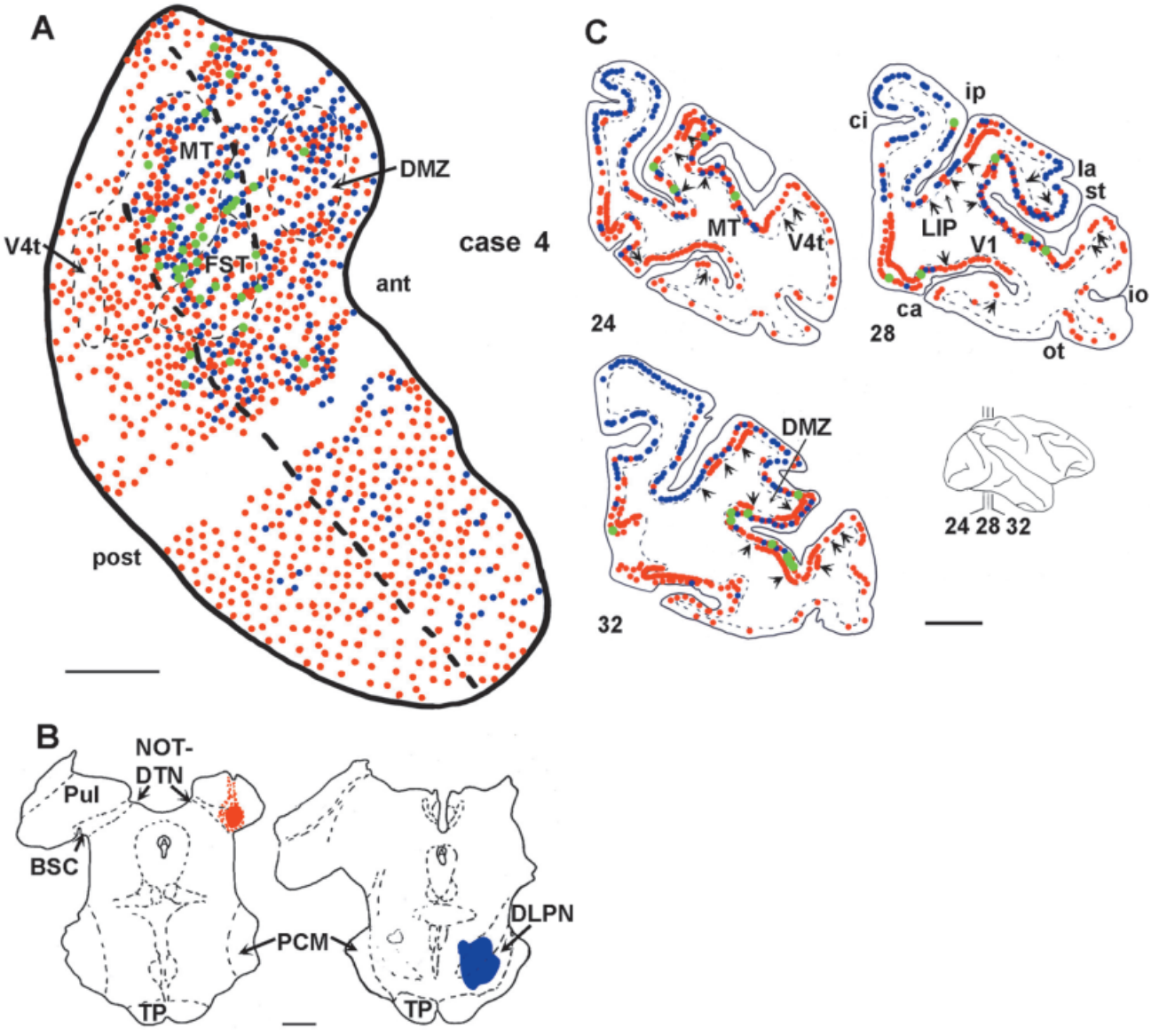


Fig. 5. Injection sites (**B**) and resulting retrogradely labeled neurons in the ipsilateral STS (**A,C**) of case 4. The two-dimensional map in this case was derived from frontal sections; the empty part of the STS represents tissue lost in blocking. For conventions, see Figure 3. ant, anterior; post, posterior. For other abbreviations, see list.

ing in the anterior bank of the central sulcus, the precentral gyrus, the arcuate sulcus, the upper bank of the principal sulcus, as well as in more moderate labeling in the orbital cortex. Labeling in the STS, however, was sparse, and especially the motion-sensitive areas MT and MST were largely devoid of label. Thus, involvement of the NRTP and neighboring medial pons in our DLPN injections should not affect our results especially for analysis of STS labeling.

## DISCUSSION

In the present study, by using dual retrograde tracer injections we were able to demonstrate the joint cortical input structures to the NOT-DTN and to the DLPN. On the whole, the cortical input to these two nuclear complexes varies considerably, with the input to the NOT-DTN originating mainly from the primarily visual areas and the motion-sensitive areas in the STS, and the input to the DLPN mainly originating from premotor and prefrontal areas in addition to the visual areas in the intraparietal, superior temporal, and medial lunate sulcus. The only consistently significant overlap of the two projection systems occurred in the posterior part of the STS including areas MT and MST and the surrounding cortex. In these cortical areas, neurons projecting to one or the other target are intermingled. Only a comparatively low percentage of double-labeled neurons were found in MT (3%) or MST (11%).

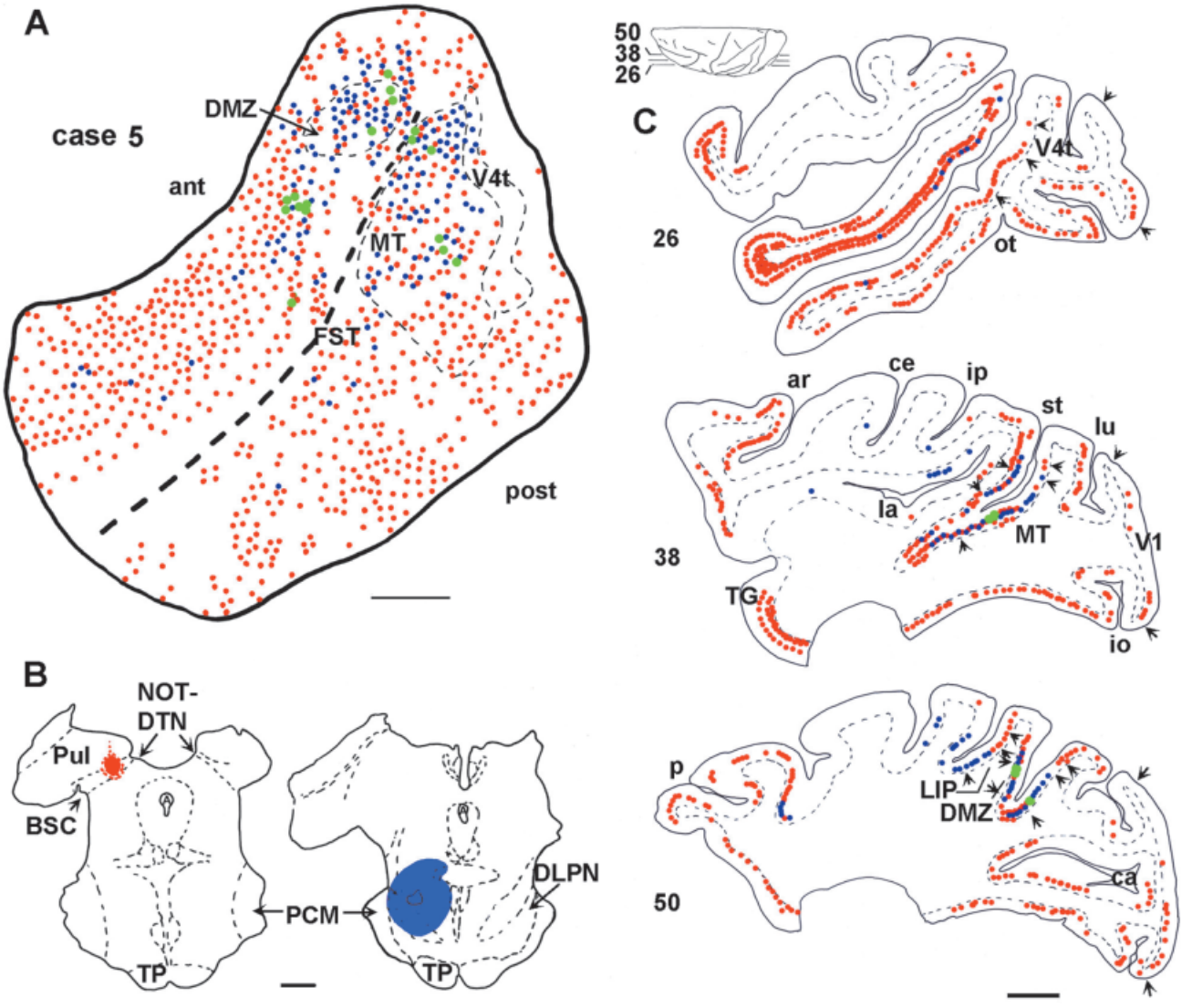


Fig. 6. Injection sites (**B**) and resulting retrogradely labeled neurons in the ipsilateral STS (**A,C**) of case 5. For conventions see Figure 3. ant, anterior; post, posterior. For other abbreviations, see list.

## Methodologic considerations

In all cases, we were able to identify double-labeled neurons in the STS, indicating that our tracer combinations were adequate to demonstrate neurons containing both tracers. By depositing the same tracer in one case in the NOT-DTN and in the other in the DLPN, we corrected the data for putative differences in uptake, transport, and overall quality of the various tracers. To quantitatively judge the prevalence of neurons projecting simultaneously to different targets in the brain, the optimal strategy is to place tracer injections into these targets that are large enough to cover the whole area but small enough to be restricted to this area. Only if the NOT-DTN and the DLPN are entirely saturated with tracer would the probability of locating double-labeled neurons reach 100%. In practice, this is accomplished only very rarely. Thus, in the present study, we combined large tracer injections that also included neighboring structures and small injections that did not involve either the entire NOT-DTN or the DLPN, respectively. With this strategy, we found between 3% and 11% of the labeled neurons in MT and MST to be double-labeled irrespective of the size of the injections (Table 3). For this reason, we did not perform control cases for which two tracers were injected into the same structure.

## Specificity of tracer injections

We recently described the areas giving rise to the cortical projection to the NOT-DTN with retrograde tracing methods (Distler and Hoffmann, 2001). The main cortical output structure was found to be MT followed by V1, V2, and V3. In these areas, retrogradely labeled cells were located in layer V only. In the present study, especially with the larger tracer injections in cases 4 and 5, additional cortical areas were labeled after NOT-DTN injection, and labeled neurons especially in these areas were

also found in layer VI. Our control injections into the pulvinar as well as data available in the literature revealed that involvement of the overlying pulvinar and medial thalamic nucleus in our NOT-DTN injections, with the exception of V1 (Lund et al., 1975), always led to bilaminar distribution of labeled cells. This property, in addition to the location of the labeled neurons, suggests that the additional label found in the prefrontal, orbital, and cingulate cortex and area TG was probably due to involvement of mainly the medial pulvinar, and in case 5 also to some spread of tracer to the area prostriata (Trojanowski and Jacobson, 1975, 1976; Mufson and Mesulam, 1984; Baleydier and Mauguiere, 1985; Levitt et al., 1995; Romanski et al., 1997; Cavada et al., 2000; Gutierrez et al., 2000; Morecroft et al., 2000). Further comparison of our NOT-DTN injections and putative spread to neighboring subdivisions of the pulvinar with data reported in other studies suggests that we did not include the main projection sites of MT that are located in the inferior and lateral pulvinar (Standage and Benevento, 1983; Ungerleider et al., 1984; Adams et al., 2000). Our injections may have included part of the projection sites from MST and FST (Boussaoud et al., 1992). Therefore, taken together, the spread of tracer to the neighboring pulvinar should not weaken our argument that the main region of overlap in NOT-DTN– and DLPN-projecting neurons and double-labeled neurons is in the posterior STS.

In this and related studies, we did not distinguish between cytoarchitectonically distinguished NOT and DTN (Büttner-Ennever et al., 1996b) but defined the physiologically defined location of retinal slip neurons typical for the NOT and the DTN as a functional unit NOT-DTN. One could argue that the small injections in our cases 2 and 3 involved the DTN, whereas the large injections of cases 4 and 5 did not. If this would be the case, one could further argue that the NOT receives cortical input from area FST but that the DTN does not. However, our database is too small to make this point, especially because the larger injections probably involved at least part of the FST- and MST-projecting sites in the pulvinar.

Similarly, our results after tracer injection into the DLPN largely correspond to the data available in the literature (e.g., Glickstein et al., 1980; Ungerleider et al., 1984; May and Andersen, 1986; Faugier-Grimaud and Ventre, 1989; Boussaoud et al., 1992; Schmahmann and Pandya, 1992; Brodal and Bjaalie, 1997). Our control injection into the NRTP suggests that spread of tracer to this nucleus did not contribute significantly to labeling in the STS.

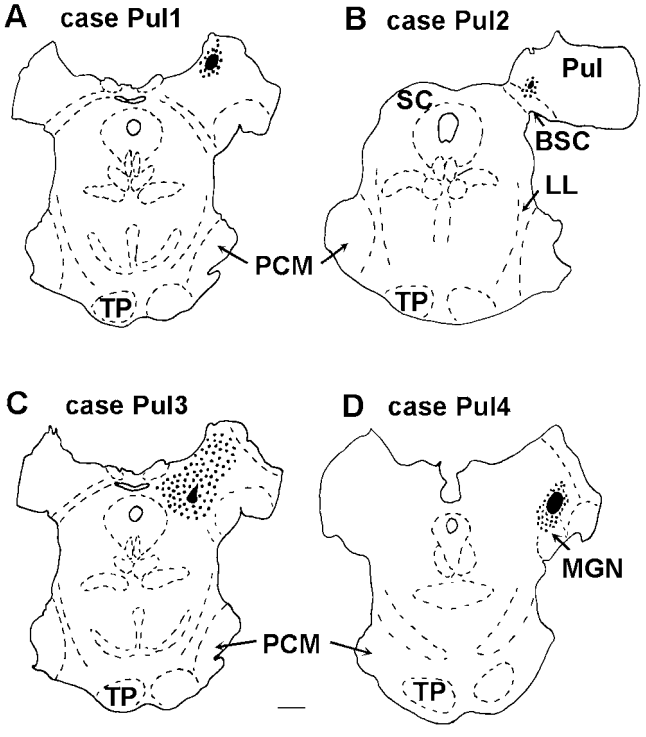


Fig. 7. Line drawings of four control injection sites into the pulvinar. The center of the injections is indicated by solid black areas, the spread of tracer is indicated by dots. For abbreviations, see list. Scale bar = 2 mm in C-D (applies to A–D).

## Functional considerations

The relative paucity of double-labeled neurons and the differential density of labeling in MT and MST associated with NOT-DTN and DLPN injections suggest that these cortical brainstem pathways may be serving somewhat different functions. Lesion studies indicate that selectively damaging or inactivating areas MT and MST produce different defects in slow eye movement. Lesions of MT mainly lead to a decrease of smooth pursuit gain for targets moving in the scotoma created by the lesion (retinotopic disorder). In contrast, MST lesions lead to both a retinotopic and directional deficit in smooth pursuit. The directional deficit is characterized as a decrease in smooth pursuit gain (eye velocity/target velocity) for movement toward the side of lesion. The initial rapid rise in eye velocity during OKN is also compromised after these lesions (Newsome et al., 1985; Duersteler and Wurtz, 1988). Differential MT and MST projections to the NOT-DTN

TABLE 4. Quantitative Assessment of Labeling Strength in Cortical Layers V and VI (Ratio = V:VI)[1]

| Case | MT | MST | FST | ant STS up. | ant STS low. |
|---|---|---|---|---|---|
| NOT-DTN2 | V only | V only | V only | 0 | 0 |
| NOT-DTN3 | V only | V only | V only | V only | V only |
| NOT-DTN4 | 1:0.52 | 1:4.67 | 1:4.4 | >1:5 | 0 |
| NOT-DTN5 | 1:0.2 | 1:0.97 | 1:0.36 | >1:4 | 0 |
| Pul1 | 1:1.25 | 1:0.35 | 1:5 | 1:0.63 | – |
| Pul2 | 1:9 | 1:3.4 | 1:13.9 | 1:24.4 | 1:53.8 |
| Pul3 | 1:0.58 | 1:3.3 | – | 1:3.7 | 1:0.97 |
| Pul4 | 1:0.43 | 1:1.64 | – | 1:3.5 | – |

[1]The table gives the average ratio of cells labeled after NOT-DTN injection in our cases 2–5 and in our pulvinar cases Pul1–4 in layer V and layer VI in various cortical areas. 0 indicates areas not analyzed, – indicates no significant label. ant STS up., upper bank of the anterior STS; ant STS low., lower bank of the anterior STS. For other abbreviations, see list.

and DLPN could support different aspects of smooth pursuit, including initiation, maintenance, and plasticity.

Neurons in both the NOT-DTN and DLPN have been identified that preferentially respond to large area random dot patterns. Such sensitivity is essential for supporting optokinetic eye movements. Similarly, neurons in both the NOT-DTN and DLPN have been discovered that respond preferentially to small diameter (<10 degrees) visual stimuli (Mustari et al., 1988; Mustari and Fuchs, 1990; Suzuki et al., 1990; Ilg and Hoffmann, 1993). These units typically have receptive fields that include the representation of the fovea, making them ideal for playing a role in smooth pursuit. Suzuki and coworkers (Suzuki et al., 1990) quantitatively compared the response properties of MT/MST neurons with those of DLPN neurons and concluded that MT and MST transmit differential input to the DLPN. A comparable study has not been done for the NOT-DTN.

In the present study, we compared the strength of the projections originating from MT and MST with the NOT-DTN and DLPN. If we set the density of retrogradely labeled cells in layer V of MT at 100%, we found that, after NOT-DTN injection, the labeling in MT was generally more dense than in MST, i.e., labeling in MST was at 38%, 111%, 75%, or 82% of that observed in MT for our respective cases. This finding confirms our earlier data where we used restricted tracer injections into the NOT-DTN and found that the most dense label always occurred in MT (Distler and Hoffmann, 2001). By contrast, after DLPN injection, the labeling in MT was less dense than in MST with labeling at 200%, 123%, 257%, or 174% of MT labeling in our respective cases. This finding indicates that the NOT-DTN receives cortical input mainly from MT and the DLPN receives its cortical input mainly from MST. The percentage of neurons projecting both to the NOT-DTN and the DLPN (double-labeled cells), however, does not systematically vary between MT and MST (Table 3). Thus, it seems that only a relatively small subpopulation of MT- and MST-neurons supplies information about moving stimuli to both NOT-DTN and DLPN, whereas the majority of this motion-sensitive cortical projection system remains segregated.

The differential cortical projections to the NOT-DTN and DLPN may be related to the efferent projections of these brainstem centers. It is well established that the NOT-DTN drives the visual climbing fiber input to the cerebellum by means of the dorsal cap of Kooy in the inferior olive. This pathway is likely to play a role in plastic changes in vestibular ocular function (Raymond and Lisberger, 1998). The NOT-DTN is known to be essential for producing optokinetic nystagmus (OKN; see Fuchs and Mustari, 1993, for review), including charging the velocity storage mechanism (Raphan et al., 1977) which generates optokinetic after-nystagmus (OKAN). The NOT-DTN could support this function by way of connections with the nucleus prepositus hypoglossi (NPH) and medial vestibular nucleus (MVN) (Mustari et al., 1994; Büttner-Ennever et al., 1996a,b). By generating OKN, the NOT-DTN supports the vestibular ocular reflex (VOR). The VOR generates eye movement that is nearly equal in magnitude and opposite in direction to head movement. The gain of the VOR (eye velocity divided by head velocity) is less than 1 when measured in darkness but reaches unity when head movements are made in the light. This enhanced VOR performance is due, at least in part, to the contribution of the NOT-DTN (Yakushin et al., 2000a). Because head movements can preferentially activate either rotational (vestibular-ocular) or translational (otolith-ocular) mechanisms, supporting rotational and translational optokinetic responses have been proposed (see Miles, 1993 for review). Miles and Busettini (1992) have suggested that the NOT-DTN contributes preferentially to rotational and the DLPN to translational optokinetic responses called ocular following (Miles, 1993). The ocular following response (OFR) is a relatively stereotyped smooth eye movement elicited within 50–60 msec of a step in full-field visual velocity (Miles et al., 1986) and shares pathways with the OKN system. Such a step in visual velocity occurs in association with head movement or saccades. In the Miles and Busettini (1992) model, "early" or "direct" pathways involving the DLPN could provide signals for initiation of the short latency ocular following response and smooth pursuit. They postulated (wrongly) that neurons in the NOT-DTN had inappropriate dynamics and connections to be involved in the "early" pathway. Rather, they modeled the NOT-DTN as contributing only to a "delayed" or "indirect" pathway, involved in velocity storage (Raphan et al., 1977). However, recent work (Kawano et al., 1996; Inoue et al., 2000) indicates that the NOT-DTN plays a role in the initiation of short latency ocular following response and smooth pursuit. The pathways used by the NOT-DTN to support this function remain to be completely established but could involve NOT-DTN connections with the DLPN, MVN, or NPH (Mustari et al., 1994; Büttner-Ennever et al., 1996a,b).

The DLPN provides a mossy fiber input to the flocculus and ventral paraflocculus of the cerebellum. This pathway can play a role in moment-by-moment control of smooth pursuit eye movements (Mustari et al., 1988; Thier et al., 1988; Mustari and Fuchs, 1990; Suzuki et al., 1990). This is because the signal controlling smooth pursuit eye movements is thought to be encoded in simple-spike discharge (driven by mossy-fiber parallel-fiber system) of floccular and ventral paraflocular Purkinje cells (Stone and Lisberger, 1990). The DLPN may also contribute to the visual-vestibular function, including providing a signal that cancels the VOR when an object of interest moves with the head. Lesion studies of the DLPN disrupt smooth pursuit, OKN, and ocular following. Lesions of the NOT-DTN, DLPN, MT, and MST all have an influence on optokinetic, ocular following, and smooth pursuit eye movements.

In conclusion, the differential input from MT and MST neurons to the NOT-DTN and DLPN may support the complimentary roles these brainstem structures play in the control of eye movements. The NOT-DTN and DLPN have differential projections to the cerebellum and brainstem supported by different populations of cortical neurons. Further studies will be necessary to define the precise role played by these complimentary pathways.

## ACKNOWLEDGMENTS

We thank E. Brockmann, H. Korbmacher, S. Krämer, A. Neff, I. Paas, G. Reuter, and G. Tinney for their expert technical assistance during the course of these experiments. This study was supported by Sonderforschungsbereich 509 of the Deutsche Forschungsgemeinschaft, a Lise-Meitner stipend to C.D., and a NIH grant to M.M.

## LITERATURE CITED


Adams MM, Hof PR, Gattass R, Webster MJ, Ungerleider LG. 2000. Visual cortical projections and chemoarchitecture of macaque monkey pulvinar. J Comp Neurol 419:377–393.

Angelucci A, Clasca F, Sur M. 1996. Anterograde axonal tracing with the subunit B of cholera toxin: a highly sensitive immunohistochemical protocol for revealing fine axonal morphology in adult and neonatal brains. J Neurosci Methods 65:101–112.

Baleydier C, Mauguiere F. 1985. Anatomical evidence for medial pulvinar connections with the posterior cingulate cortex, the retrosplenial area, and the posterior parahippocampal gyrus in monkeys. J Comp Neurol 232:219–228.

Ballas I, Hoffmann K-P. 1985. A correlation between receptive field properties and morphological structures in the pretectum of the cat. J Comp Neurol 238:417–428.

Boussaoud D, Desimone R, Ungerleider LG. 1992. Subcortical connections of visual areas MST and FST in macaques. Vis Neurosci 9:291–302.

Brodal P, Bjaalie JG. 1997. Salient anatomic features of the cortico-pontocerebellar pathway. Prog Brain Res 114:227–249.

Brückner G, Seeger G, Brauer K, Härtig W, Kacza J, Bigl V. 1994. Cortical areas are revealed by distribution patterns of proteoglycan components and parvalbumin in the mongolian gerbil and rat. Brain Res 658:67–86.

Büttner-Ennever JA, Cohen B, Horn AKE, Reisine H. 1996a. Pretectal projections to the oculomotor complex of the monkey and their role in eye movements. J Comp Neurol 366:348–359.

Büttner-Ennever JA, Cohen B, Horn AKE, Reisine H. 1996b. Efferent pathways of the nucleus of the optic tract in monkey and their role in eye movements. J Comp Neurol 373:90–107.

Cavada C, Company T, Tejedor J, Cruz-Rizzolo RJ, Reinoso-Suarez F. 2000. The anatomical connections of the macaque monkey orbitofrontal cortex (review). Cereb Cortex 10:220–242.

Distler C, Hoffmann K-P. 2001. Cortical input to the nucleus of the optic tract and dorsal terminal nucleus (NOT-DTN) in macaques: a retrograde tracing study. Cereb Cortex 11:572–580.

Distler C, Boussaoud D, Desimone R, Ungerleider LG. 1993. Cortical connections of inferior temporal area TEO in macaque monkeys. J Comp Neurol 334:125–150.

Duersteler MR, Wurtz RH. 1988. Pursuit and optokinetic deficits following chemical lesions of cortical areas MT and MST. J Neurophysiol 60:940–965.

Faugier-Grimaud S, Ventre J. 1989. Anatomic connections of inferior parietal cortex (area 7) with subcortical structures related to vestibulo-ocular function in a monkey (Macaca fascicularis). J Comp Neurol 280:1–14.

Fuchs AF, Mustari MJ. 1993. The optokinetic response in primates and its possible neuronal substrate. Rev Oculomot Res 5:343–369.

Gallyas F. 1979. Silver staining of myelin by means of physical development. Neurol Res 1:203–209.

Glickstein M, Cohen JL, Dixon B, Gibson A, Hollins M, Labossiere E, Robinson F. 1980. Corticopontine visual projections in macaque monkeys. J Comp Neurol 190:209–229.

Grasse KL, Cynader MS. 1984. Electrophysiology of lateral and dorsal terminal nuclei of the cat accessory optic system. J Neurophysiol 51: 276–293.

Gutierrez C, Cola MG, Seltzer B, Cusick C. 2000. Neurochemical and connectional organization of the dorsal pulvinar complex in monkeys. J Comp Neurol 419:61–86.

Hess DT, Merker BH. 1983. Technical modifications of Gallyas' silver stain for myelin. J Neurosci Methods 8:95–97.

Hof PR, Morrison JH. 1995. Neurofilament protein defines regional patterns of cortical organization in the macaque monkey visual system: a quantitative immunohistochemical analysis. J Comp Neurol 352:161–186.

Hoffmann K-P, Distler C. 1989. Quantitative analysis of visual receptive fields of neurons in the nucleus of the optic tract and dorsal terminal nucleus of the accessory optic tract in macaque monkey. J Neurophysiol 62:416–428.

Hoffmann K-P, Fischer WH. 2001. Directional effect of inactivation of the nucleus of the optic tract on optokinetic nystagmus in the cat. Vision Res 41:3389–3398.

Hoffmann K-P, Schoppmann A. 1975. Retinal input to direction selective cells in the nucleus of the optic tract of the cat. Brain Res 99:359–366.

Hoffmann K-P, Distler C, Erickson R, Mader W. 1988. Physiological and anatomical identification of the nucleus of the optic tract and dorsal terminal nucleus of the accessory optic tract in monkeys. Exp Brain Res 69:635–644.

Hoffmann K-P, Distler C, Ilg U. 1992. Cortical contributions to ipsilateral field representation and direction selectivity in the macaque monkey's nucleus of the optic tract and dorsal terminal nucleus. J Comp Neurol 321:150–162.

Hoffmann K-P, Distler C, Bremmer F, Thiele A. 2002. Directional asymmetry of neurons in cortical areas MT and MST projecting to the nucleus of the optic tract and dorsal terminal nucleus (NOT-DTN) in macaques. J Neurophysiol (in press).

Ilg UJ, Hoffmann K-P. 1991. Responses of monkey nucleus of the optic tract neurons during pursuit and fixation. Neurosci Res 12:101–110.

Ilg UJ, Hoffman K-P. 1993. Functional grouping of the cortico-pretectal projection. J Neurophysiol 70:867–869.

Ilg UJ, Bremmer F, Hoffmann K-P. 1993. Optokinetic and pursuit system: a case report. Behav Brain Res 57:21–29.

Inoue Y, Takemura A, Kawano K, Mustari MJ. 2000. Role of the pretectal nucleus of the optic tract in short-latency ocular following responses in monkeys. Exp Brain Res 131:269–281.

Kato I, Harada K, Hasekawa K, Koike Y. 1988. Role of the nucleus of the optic tract in monkeys in optokinetic nystagmus and optokinetic after-nystagmus. Brain Res 474:16–26.

Kawano K, Shidara M, Yamane S. 1992. Neural activity in dorsolateral pontine nucleus of alert monkey during ocular following responses. J Neurophysiol 67:680–703.

Kawano K, Shidara M, Watanabe Y, Yamane S. 1994. Neural activity in cortical area MST of alert monkey during ocular following responses. J Neurophysiol 71:2305–2324.

Kawano K, Takemura A, Inoue Y, Kitama T, Kobayashi Y, Mustari MJ. 1996. Visual inputs to cerebellar ventral paraflocculus during ocular following responses. Prog Brain Res 112:415–422.

Komatsu H, Wurtz RH. 1988. Relation of cortical areas MT and MST to pursuit eye movements. I. Localization and visual properties of neurons. J Neurophysiol 60:580–603.

Levitt JB, Yoshioka T, Lund JS. 1995. Connections between the pulvinar complex and cytochrome oxidase-defined compartments in visual area V2 of macaque monkey. Exp Brain Res 104:419–430.

Lund JS, Lund RD, Hendrickson AE, Bunt AH, Fuchs AF. 1975. The origin of efferent pathways from the primary visual cortex, area 17, of the macaque monkey as shown by retrograde transport of horseradish peroxidase. J Comp Neurol 164:287–304.

Maunsell JHR, Van Essen DC. 1983. The connections of the middle temporal visual area (MT) and their relationship to a cortical hierarchy in the macaque monkey. J Neurosci 3:2563–2586.

May JG, Andersen RA. 1986. Different patterns of corticopontine projections from separate cortical fields within the inferior parietal lobule and dorsal prelunate gyrus of the macaque. Exp Brain Res 63:265–278.

May JG, Keller EL, Suzuki DA. 1988. Smooth pursuit eye movement deficits with chemical lesions in the dorsolateral pontine nucleus of the monkey. J Neurophysiol 59:952–977.

Miles FA. 1993. The sensing of rotational and translational optic flow by the primate optokinetic system. Rev Oculomot Res 5:393–403.

Miles FA, Busettini C. 1992. Ocular compensation for self-motion: visual mechanisms. Sensing and controlling motion. Ann N Y Acad Sci 656: 220–232.

Miles FA, Kawano K, Optican LM. 1986. Short-latency ocular following responses of monkey. I. Dependence on temporospatial properties of visual input. J Neurophysiol. 56:1321–1354.

Morecroft RJ, Rockland KS, Van Hoesen GW. 2000. Localization of area prostriata and its projection to the cingulate motor cortex in the rhesus monkey. Cereb Cortex 10:192–203.

Mufson EJ, Mesulam MM. 1984. Thalamic connections of the insula in the rhesus monkey and comments on the paralimbic connectivity of the medial pulvinar nucleus. J Comp Neurol 227:109–120.

Mustari MJ, Fuchs AF. 1990. Discharge patterns of neurons in the pretectal nucleus of the optic tract (NOT) in the behaving primate. J Neurophysiol 64:77–90.

Mustari MJ, Fuchs AF, Wallman J. 1988. Response properties of dorsolateral pontine units during smooth pursuit in the rhesus macaque. J Neurophysiol 60:664–686.

Mustari MJ, Fuchs AF, Kaneko CR, Robinson FR. 1994. Anatomical connections of the primate pretectal nucleus of the optic tract. J Comp Neurol 349:111–128.

Mustari MJ, Fuchs AF, Pong M. 1997. The response properties of pretectal omnidirectional pause neurons in the behaving primate. J Neurophysiol 77:116–125.

Newsome WT, Wurtz RH, Duersteler MR, Mikami A. 1985. Deficits in visual motion processing following ibotenic acid lesions of the middle temporal visual area of the macaque monkey. J Neurosci 5:825–840.

Raphan T, Cohen B, Matsuo V. 1977. A velocity storage mechanism responsible for optokinetic nystagmus (OKN), optokinetic after nystagmus (OKAN) and vestibular nystagmus. Dev Neurosci 1:37–47.

Raymond J, Lisberger SG. 1998. Neural learning rules for the vestibular ocular reflex. J Neurosci 18: 9112–9129.

Romanski LM, Giguere M, Bates JF, Goldman-Rakic PS. 1997. Topographic organization of medial pulvinar connections with the prefrontal cortex in the rhesus monkey. J Comp Neurol 379:313–332.

Schiff D, Cohen B, Raphan T. 1988. Nystagmus induced by stimulation of the nucleus of the optic tract in the monkey. Exp Brain Res 70:1–14.

Schiff D, Cohen B, Büttner-Ennever J, Matsuo V. 1990. Effects of lesions of the nucleus of the optic tract on optokinetic nystagmus and after-nystagmus in the monkey. Exp Brain Res 79:225–239.

Schmidt M. 1996. Neurons in the cat pretectum that project to the dorsal lateral geniculate nucleus are activated during saccades. J Neurophysiol 76:2907–2918.

Schmahmann JD, Pandya DN. 1992. Course of the fiber pathways to pons from parasensory association areas in the rhesus monkey. J Comp Neurol 326:159–179.

Standage GP, Benevento LA. 1983. The organization of connections between the pulvinar and visual area MT in the macaque monkey. Brain Res 262:288–294.

Stone LS, Lisberger SG. 1990. Visual responses of Purkinje cells in the cerebellar flocculus during smooth pursuit eye movements in monkeys. II. Complex spikes. J Neurophysiol 63:1262–1275.

Sudkamp S, Schmidt M. 1995. Physiological characterization of pretectal neurons projecting to the lateral posterior-pulvinar complex in the cat. Eur J Neurosci 7:881–888.

Suzuki DA, Keller EL. 1984. Visual signals in the dorsolateral pontine nucleus of the alert monkey: their relationship to smooth-pursuit eye movements. Exp Brain Res 47:145–147.

Suzuki DA, May JG, Keller EL, Yee RD. 1990. Visual motion response properties of neurons in dorsolateral pontine nucleus of alert monkey. J Neurophysiol 63:37–59.

Taylor RB, Wennberg RA, Lozano AM, Sharpe JA. 2000. Central nystagmus induced by deep-brain stimulation for epilepsy. Epilepsia 41: 1637–1641.

Thiele A, Bremmer F, Ilg UJ, Hoffmann K-P. 1997. Visual responses of neurons from areas V1 and MT in a monkey with late onset strabismus: a case study. Vision Res 37:853–863.

Thier P, Koehler W, Buettner UW. 1988. Neuronal activity in the dorsolateral pontine nucleus of the alert monkey modulated by visual stimuli and eye movements. Exp Brain Res 70:496–512.

Thier P, Bachor A, Faiss J, Dichgans J, Koenig E. 1991. Selective impairment of smooth pursuit eye movements due to an ischemic lesion of the basal pons. Ann Neurol 29:443–448.

Trojanowski JQ, Jacobson S. 1975. A combined horseradish peroxidase-autoradiographic investigation of reciprocal connections between superior temporal gyrus and pulvinar in squirrel monkey. Brain Res 85: 347–353.

Trojanowski JQ, Jacobson S. 1976. Areal and laminar distribution of some pulvinar cortical efferents in rhesus monkey. J Comp Neurol 169:371–392.

Ungerleider LG, Galkin TW, Mishkin M. 1983. Visuotopic organization of projections from striate cortex to inferior and lateral pulvinar in rhesus monkey. J Comp Neurol 217:137–157.

Ungerleider LG, Desimone R, Galkin TW, Mishkin M. 1984. Subcortical projections of area MT in the macaque. J Comp Neurol 223:368–386.

van der Want JJL, Klooster J, Nunes Cardozo B, de Weerd H, Liem RSB. 1997. Tract-tracing in the nervous system of vertebrates using horseradish peroxidase and its conjugates: tracers, chromogens, and stabilization for light and electron microscopy. Brain Res Protocols 1:269–279.

Van Essen DC, Maunsell JHR. 1980. Two-dimensional maps of the cerebral cortex. J Comp Neurol 191:255–281.

Yakushin SB, Reisine H, Büttner-Ennever J, Raphan T, Cohen B. 2000a. Functions of the nucleus of the optic tract (NOT). I. Adaptation of the gain of the horizontal vestibulo-ocular reflex. Exp Brain Res 131:416–432.

Yakushin SB, Gizzi M, Reisine H, Raphan T, Büttner-Ennever J, Cohen B. 2000b. Functions of the nucleus of the optic tract (NOT). II. Control of ocular pursuit. Exp Brain Res 131:433–447.